

Crystal Structure and Ionic Conductivity of $\text{Na}_2\text{Mg}_2(\text{PO}_3)_3\text{N}$ Mi-Sun Lee,[†] Jun-Kun Kang,[‡] and Seung-Joo Kim^{†,*,‡}[†]Department of Chemistry, Division of Energy Systems Research, Ajou University, Suwon 443-749, Korea
^{*}E-mail: sjookim@ajou.ac.kr[‡]Institute of NT-IT Fusion Technology, Ajou University, Suwon 443-749, Korea
Received February 7, 2012, Accepted March 19, 2012**Key Words** : X-ray diffraction, Crystal structure, Ionic conductivity, Nitridooxophosphates

Inorganic nitridooxophosphates have been of interest because of their novel structural aspects and physical properties different from oxophosphates. In typical oxophosphates, pentavalent phosphorous atom is coordinated to four oxygen atoms to form a PO_4 tetrahedron. The oxygen atoms can be connected to either one phosphorous tetrahedron center, as terminal atoms, or to two phosphorous tetrahedron centers, as simple bridging atoms. By contrast, the nitrogen atoms in nitridooxophosphates have been found as three kinds of forms: (i) terminal atoms, (ii) simple bridging atoms connected to two tetrahedra, and (iii) triply-bridging atoms connected to three tetrahedra. The presence of triply-bridging nitrogen can provide with a more tightly linked $\text{P}(\text{O},\text{N})_4$ network, resulting in the improvements of hardness, refractive index and chemical durability.^{1,2} For this reason, the nitridation of oxophosphates has been proved as an effective way for exploring new materials applicable to various fields such as optical materials, catalysts and solid electrolytes, *etc.*³⁻⁵

More than two decades ago, W. Feldmann reported the synthesis of several isotypic compounds with the chemical formulae of $\text{A}_3\text{B}(\text{PO}_3)_3\text{N}$ ($\text{A}^+ = \text{Na}, \text{K}; \text{B}^{3+} = \text{Al}, \text{Ga}, \text{Cr}, \text{Mn}, \text{Fe}$) and $\text{A}_2\text{B}_2(\text{PO}_3)_3\text{N}$ ($\text{A}^+ = \text{Na}; \text{B}^{2+} = \text{Mg}, \text{Mn}, \text{Fe}, \text{Co}$) by versatile nitridation reactions.⁶⁻⁸ The crystal structure of $\text{Na}_3\text{AlP}_3\text{O}_9\text{N}$ has been determined by X-ray diffraction on a single-crystal.⁹ For other compounds, however, no information except their cell parameters has been known. In this work, we report the crystal structure of $\text{Na}_2\text{Mg}_2(\text{PO}_3)_3\text{N}$ from Rietveld refinement based on powder X-ray diffraction data and bond valence sum calculation. We also discuss the ionic conductivity of $\text{Na}_2\text{Mg}_2(\text{PO}_3)_3\text{N}$. There are no reports so far, to our knowledge, on measurements of ionic conductivity for the sodium-containing nitridooxophosphates.

$\text{Na}_2\text{Mg}_2(\text{PO}_3)_3\text{N}$ was synthesized by the thermal nitridation of stoichiometric mixture of NaPO_3 , MgO and $\text{NH}_4\text{H}_2\text{PO}_4$ in flowing ammonia gas at 800 °C. The powder X-ray diffraction patterns for $\text{Na}_2\text{Mg}_2(\text{PO}_3)_3\text{N}$ showed the cubic symmetry with lattice parameter $a = 9.24119(10)$ Å, which is accordance with the previously reported value.⁶ No additional peaks due to impurity phase were observed at the resolution limit of the instrument. Systematic absences, $h = 2n+1$ for $h00$ observed in the intensity data, suggested the space group of $P2_13$. As an initial model for Rietveld refinement, we adopted the structural parameters of a single

crystal $\text{Na}_3\text{Al}(\text{PO}_3)_3\text{N}$.⁹ Refinement of atomic positions and isotropic displacement parameters were carried out using the Fullprof program package with pseudo-Voigt peak shapes.¹⁰ The background was fitted using a linear interpolation function with manually selected points. The isotropic thermal parameters for O1, O2 and O3 were constrained to be equal. The structure parameters (unit cell parameters,

Table 1. Unit cell parameters and atomic coordinates for $\text{Na}_2\text{Mg}_2(\text{PO}_3)_3\text{N}$ refined from X-ray powder diffraction ($\lambda = 1.5419$ Å)

Space group $P2_13$ (No. 198)					
$a = 9.24119(10)$ Å, $V = 789.20(2)$ Å ³ , $Z = 4$					
$R_p = 6.81\%$, $R_{wp} = 10.1\%$, $R_{exp} = 7.66\%$, $R_{Bragg} = 3.54\%$, $\chi^2 = 1.75$					
Atom	Position	x	y	z	B_{iso}
P1	12b	0.3424(3)	0.0917(3)	0.2604(4)	1.16(5)
Mg1	4a	0.5785(3)	0.5785(3)	0.5785(3)	0.82(13)
Mg2	4a	0.3956(5)	0.3956(5)	0.3956(5)	1.31(14)
Na1	4a	0.0367(3)	0.0367(3)	0.0367(3)	1.08(14)
Na2	4a	0.7923(4)	0.7923(4)	0.7923(4)	1.7(2)
O1	12b	0.2251(7)	0.0176(6)	0.8686(5)	1.20(9)
O2	12b	0.4009(6)	0.0046(6)	0.1329(5)	1.20(9)
O3	12b	0.4574(6)	0.1934(5)	0.3283(6)	1.20(9)
N1	4a	0.1956(6)	0.1956(6)	0.1956(6)	1.5(3)

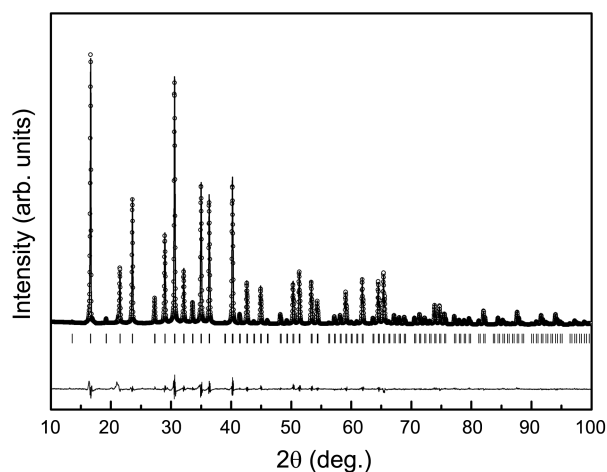
**Figure 1.** Observed (open circles), calculated (line) and difference (bottom) X-ray diffraction patterns for $\text{Na}_2\text{Mg}_2(\text{PO}_3)_3\text{N}$. Vertical bars indicate calculated positions of Bragg peaks.

Table 2. Selected bond distances (Å) and angles (°) for Na₂Mg₂(PO₃)₃N

Na ₂ Mg ₂ (PO ₃) ₃ N			
P coordination		Mg coordination	
P–O1	1.551(6)	Mg1–O1	1.962(7) × 3
P–O2	1.527(6)	Mg1–O2	2.078(6) × 3
P–O3	1.551(6)	O1–Mg1–O1	96.1(5)
P–N	1.766(6)	O1–Mg1–O2	90.7(4), 93.2(4)
		O2–Mg1–O2	78.9(4)
		Mg2–O2	2.150(7) × 3
Na coordination		Mg2–O3	
Na1–O1	2.340(7) × 3	O2–Mg2–O2	75.8(4)
Na1–O3	2.870(6) × 3	O2–Mg2–O3	91.4(4), 98.4(4)
Na1–N	2.543(6)	O3–Mg2–O3	93.5(4)
Na2–O1	2.946(7) × 3		
Na2–O2	3.002(7) × 3		
Na2–O3	2.340(6) × 3		

refined atomic positions and isotropic temperature factors) and residual indices are summarized in Table 1. The observed, calculated and difference patterns from the Rietveld refinements plots for XPD are shown in Figure 1. Selected interatomic distances and bond angles from the refined crystal structure are given in Table 2.

In the present structural model, phosphorous and oxygen atoms lie on general positions (12b) and the other atoms lie on the special positions with three fold axis (4a). Sodium, magnesium and nitrogen atoms are arranged along [111] direction in the sequence of Mg1–Mg2–N–Na1–Na2–Mg1–... Sodium and magnesium atoms with similar X-ray scattering factors have the same site symmetry in this structure. Moreover, oxygen and nitrogen atoms also have similar X-ray scattering factors. Hence, the Na/Mg/N distribution in Na₂Mg₂(PO₃)₃N lattice was examined with Bond Valence Sum (*BVS*) calculations.¹¹ The *BVS* rule states that the formal charge (*V*) of a cation (anion) must be equal to the sum of the bond valences (*s*) around this cation (anion). The deviation between formal charge and bond valence sum can be quantified by means of a global instability index (*GII*) and used as a measure of the instability or the inadequacy of the structure.¹² The smallest *GII* value (6.3%) was obtained from the present model (Table 3). For other arrangement, for instance, such as Mg1–Na1–N–Mg2–Na2–Mg1-, the *GII*

Table 3. Bond Valence Sums (*V**), the formal charges (*V*) and Global Instability Index (*GII*) for Na₂Mg₂(PO₃)₃N

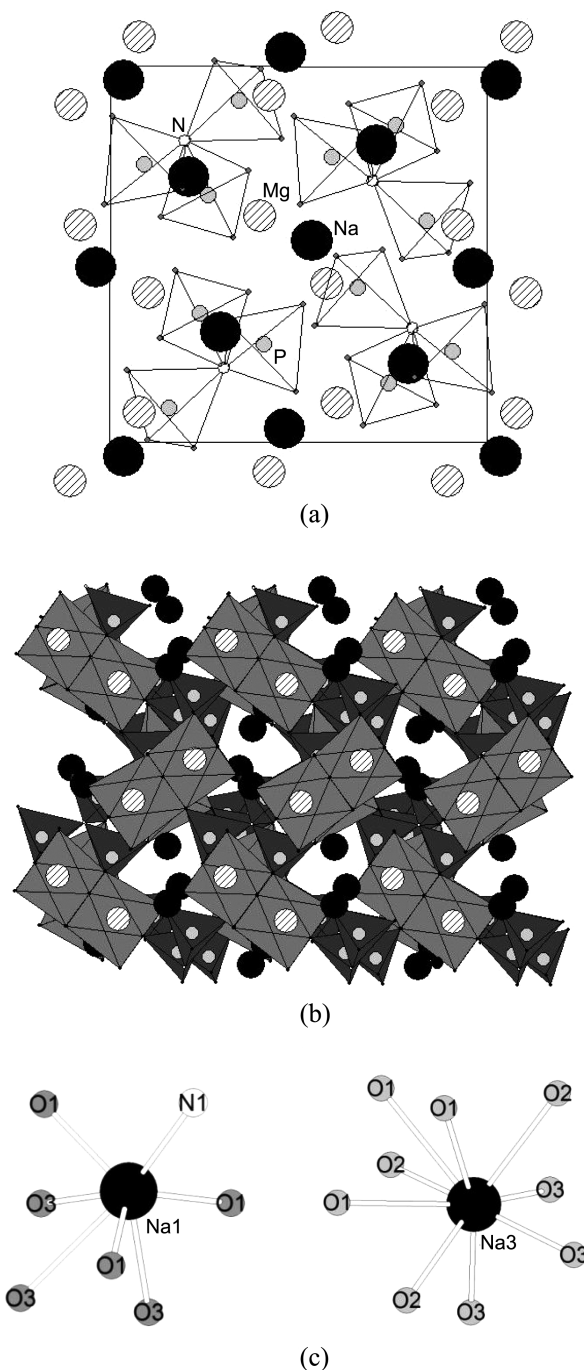
Atoms	<i>V</i> *	<i>V</i>	Atoms	<i>V</i> *	<i>V</i>
Na1	1.061	1	O1	1.998	2
Na2	0.957	1	O2	1.919	2
Mg1	2.510	2	O3	1.865	2
Mg2	2.012	2	N1	2.728	3
P	4.512	5			

*GII** 6.33%

$$*GII = \frac{\sum(|V^* - V| \times \text{multiplicity}/V)}{\text{Number of Atoms in unit cell}}$$

value significantly increased up to about 19%.

In the structure of Na₂Mg₂(PO₃)₃N, phosphorous atom is coordinated to three oxygen atoms and one nitrogen atom to form a PO₃N tetrahedron. The (PO₃)₃N entity is formed by three PO₃N tetrahedra sharing the corner occupied by the nitrogen atom (Figure 2(a)). The P–O bond lengths (1.53–1.55 Å) in Na₂Mg₂(PO₃)₃N are close to those found in the compositional analogues such as Na₃Al(PO₃)₃N (1.50–1.52 Å)⁹ and Na₄Mg₃(PO₄)(P₂O₇)₃ (1.54 Å).¹³ The P–N bond length

**Figure 2.** (a) Schematic views of the structure of Na₂Mg₂(PO₃)₃N showing the (PO₃)₃N entity. (b) Polyhedral views along [110] direction showing the Na-containing tunnels. (c) Local coordination around Na1 and Na2 atoms.

(1.77 Å) is similar to those observed for the tricoordinated nitrogen atoms in nitrido-compounds such as $K_3P_6N_{11}$ (1.71 Å).¹⁴ The magnesium atoms occupy two nonequivalent sites. Each magnesium atom is connected to six oxygen atoms located at the vertexes of PO_3N tetrahedra, forming a distorted octahedron. The MgO_6 octahedron is connected to other MgO_6 octahedron with face-sharing. Hence, the structure of $Na_2Mg_2(PO_3)_3N$ can be considered as a three dimensional network consisting of $(PO_3)_3N$ entities bridged by magnesium atoms. It is worthy to note that large tunnels are extended along the three main crystallographic directions $\langle 110 \rangle$, $\langle 011 \rangle$, and $\langle 101 \rangle$, where sodium atoms are located. (Figure 2(b)) Sodium atoms occupy two different crystallographic positions. Na1 is bonded to six oxygens and one nitrogen, while Na2 is coordinated to nine oxygens. The local structures around the sodium atoms are irregular as shown in Figure 2(c). The highly distorted environment of the sodium atoms in $Na_2Mg_2(PO_3)_3N$ is consistent with the ^{23}Na MAS-NMR study performed previously.¹⁵

Figure 3(a) depicts the alternating current (ac) impedance measurement performed on the $Na_2Mg_2(PO_3)_3N$ in the temperature range of 400–650 °C. The bulk resistances are measured from the intercept of the low-frequency end of the semi-circle with the real axis of the complex impedance plot.

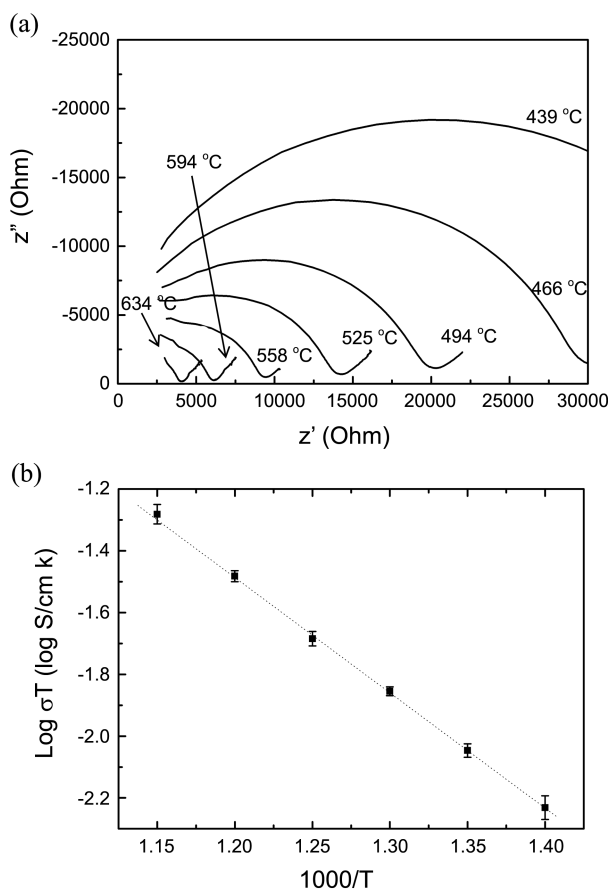


Figure 3. (a) Complex impedance diagrams at various temperatures and (b) Reciprocal temperature dependence of the ac conductivity for $Na_2Mg_2(PO_3)_3N$. Error bars represent standard deviations in the measurements at given temperatures.

The ac conductivity values plotted against reciprocal temperature shows that the relation between specific conductivity and temperature is given by the Arrhenius expression in the form: $\log \sigma T = \log \sigma_0 - E_a/RT$, where E_a is the activation energy involved in the transport process, σ_0 is a constant, and T is the absolute temperature. The good linearity observed in Figure 3(b) reflects the hopping motions of the sodium ions.¹⁶ The activation energy, 0.78 eV and the ionic conductivity ($8.2 \times 10^{-6} S cm^{-1}$ at 440 °C) for $Na_2Mg_2(PO_3)_3N$ are comparable to that for a gallia-rutile intergrowths type sodium ion conductor, $Na_{0.7}Ga_{4.7}Ti_{0.3}O_8$ ($E_a = 0.75 eV$, $\sigma = 1.0 \times 10^{-5} S cm^{-1}$ at 440 °C).¹⁷

In conclusion, it was found by means of Rietveld analysis and bond valence sum calculation that $Na_2Mg_2(PO_3)_3N$ has a three dimensional network structure consisting of $(PO_3)_3N$ groups bridged by magnesium and sodium atoms. The structure contains tunnels along the $\langle 110 \rangle$, $\langle 011 \rangle$, and $\langle 101 \rangle$ directions in which the Na^+ ions are located. The open framework of the title compound and the location of the sodium ions in its large tunnels make it a possible candidate for ionic conductivity. Although the ionic conductivity of $Na_2Mg_2(PO_3)_3N$ is still 2–3 orders of magnitude lower than NASICON-type fast ion conductors such as $NaM_2(PO_4)_3$ ($M = Ti, Zr$),^{18,19} the results of this study indicate the opportunity for additional investigations in order to explore new ionic conductor with high performance.

Experimentals

A polycrystalline sample of $Na_2Mg_2(PO_3)_3N$ was prepared by mixing a 2:2:1 molar ratio of $NaPO_3$ (Sigma Adrich, 99.9%), MgO (Sigma Adrich, 99.9%), and $NH_4H_2PO_4$ (Sigma Adrich, 99.9%). The reaction mixture was loaded to an alumina crucible and heated at 1073 K for 12 h under ammonia gas flow (flow rate = 30 mL/min) in a tube furnace.

Phase purity and structure of the final product were characterized by a powder X-ray diffraction analysis with $Cu K\alpha$ radiation ($\lambda = 1.5405 \text{ \AA}$) on a Rigaku DMAX-2200PC X-ray diffractometer. A graphite monochromator was used for diffracted beams. A step scan mode was adopted in the 2θ range of 10–100° with a scanning step of 0.02° and a sampling time of 5 seconds at the condition of 40 kV and 30 mA.

The composition of sample was confirmed with energy-dispersive X-ray analysis (JEOL JSM-5600 scanning electron microscope fitted with a Be window detector, Oxford Instrument). The ratio of atoms was matched with the nominal composition within the experimental error range (within 5% for cations and 10% for anions).

The sodium ionic conductivity measurement was performed using ac impedance spectroscopy in the range 5 Hz–13 MHz (Hewlett Packard 4192A Impedance Analyzer). For the measurement, as-prepared $Na_2Mg_2(PO_3)_3N$ sample was well ground and pressed into pellets with 12.5 mm diameter and 1.0 mm thickness. The pellets were re-heated for 6 h at 1073 K under ammonia gas flow. Sodium ion blocking electrodes were attached to the pellets using Ag paste and

the pellets fired at 473 K for 1 day, to give electrical contact between sample and electrode. The sample was equilibrated for 1-2 h and then, measured three times at each temperature. The conductivity is determined using $\sigma = (d/A)/R$, where d is the film thickness, A the area of the metal contact, and R the film resistance determined from the complex impedance plots.

Acknowledgments. This work was supported by the National Research Foundation of Korea (NRF) grant funded by the Korea government (No. 2011-0030745 and No. 2011-0005283).

References

1. Grand, T.; Holloway, J. R.; McMillan, P. F.; Angell, C. A. *Nature* **1994**, *369*, 43.
2. Marchand, R.; Laurent, Y. *Eur. J. Solid State Inorg. Chem.* **1991**, *28*, 57.
3. Benitez, J. J.; Odriozola, J. A.; Marchand, R.; Laurent, Y.; Grange, P. *J. Chem. Soc. Faraday Trans.* **1995**, *91*, 4477.
4. Fripiat, N.; Grange, P. *J. Chem. Soc. Chem. Comm.* **1996**, 1409.
5. Wang, B.; Kwak, B. S.; Sales, B. C.; Bates, J. B. *J. Non-Crystal. Solids* **1995**, *183*, 297.
6. Feldmann, W. *Z. Chem.* **1987**, *27*, 100.
7. Feldmann, W. *Z. Chem.* **1987**, *27*, 182.
8. Conanec, R.; Feldmann, W.; Marchand, R.; Laurent, Y. *J. Solid State Chem.* **1996**, *121*, 418.
9. Conanec, R.; L'Haridon, P.; Feldmann, W.; Marchand, R.; Laurent, Y. *Eur. J. Solid State Inorg. Chem.* **1994**, *31*, 13.
10. Rodriguez-Carvajal, J. *Fullprof 2000: A Rietveld Refinement and Pattern Matching Analysis Program, April 2008, Laboratoire Léon Brillouin (CEA-CNRS)*.
11. Brese, N. E.; O'Keeffe, M. *Acta Cryst. B* **1991**, *47*, 192-197.
12. Brown, I. D. *Z. Kristallogr.* **1992**, *199*, 255.
13. Essehli, R.; El Balia, B.; Benmokhtar, S.; Fuess, H.; Svobodac, I.; Obbade, S. *J. Alloys Comp.* **2010**, *493*, 654.
14. Jacobs, H.; Nymwegen, R. *Z. Anorg. Allg. Chem.* **1997**, *623*, 429.
15. Missiot, D.; Conanec, R.; Feldmann, W.; Marchand, R.; Laurent, Y. *Inorg. Chem.* **1996**, *35*, 4959.
16. Funke, K. *Prog. Solid State Chem.* **1993**, *22*, 111.
17. Edwards, D. D.; Empie, N. H.; Meethong, N.; Amoroso, J. W. *Solid State Ionics* **2006**, *177*, 1897.
18. Winand, J. M.; Rulmont, A.; Tarte, P. *J. Solid State Chem.* **1991**, *93*, 341.
19. Anantharamulu, N.; Rao, K. K.; Radha, V.; Vithal, M. *J. Mater. Sci.* **2011**, *46*, 2821-2837.